ISSN 2472-1972

Long-Acting and Selective Oxytocin Peptide Analogs Show Antidiabetic and Antiobesity Effects in Male Mice

Brandy Snider,[1] Andrea Geiser,[2] Xiao-peng Yu,[1] Emily Cathleen Beebe,[1] Jill Amanda Willency,[1] Keyun Qing,[1] Lili Guo,[2] Jianliang Lu,[3] Xiaojun Wang,[1] Qian Yang,[1] Alexander Efanov,[1] Andrew Charles Adams,[1] Tamer Coskun,[1] Paul Joseph Emmerson,[1] Jorge Alsina-Fernandez,[2] and Minrong Ai[1]

[1]Diabetes and Complications, Lilly Research Laboratories, Eli Lilly and Company, Indianapolis, Indiana 46285; [2]Biotechnology Peptide Group, Lilly Research Laboratories, Eli Lilly and Company, Indianapolis, Indiana 46285; and [3]Medicinal Chemistry, Lilly Research Laboratories, Eli Lilly and Company, Indianapolis, Indiana 46285

ORCiD numbers: 0000-0002-4629-4281 (E. C. Beebe); 0000-0002-2531-7958 (M. Ai).

Oxytocin (OXT) has been shown to suppress appetite, induce weight loss, and improve glycemic control and lipid metabolism in several species, including humans, monkeys, and rodents. However, OXT's short half-life in circulation and lack of receptor selectivity limit its application and efficacy. In this study, we report an OXT peptide analog (OXT^{Gly}) that is potent and selective for the OXT receptor (OXTR). OXT, but not OXT^{Gly}, activated vasopressin receptors *in vitro* and acutely increased blood pressure *in vivo* when administered IP. OXT suppressed food intake in mice, whereas OXT^{Gly} had a moderate effect on food intake when administered IP or intracerebroventricularly. Both OXT (IP) and OXT^{Gly} (IP) improved glycemic control in glucose tolerance tests. Additionally, both OXT (IP) and OXT^{Gly} (IP) stimulated insulin, glucagon-like peptide 1, and glucagon secretion in mice. We generated lipid-conjugated OXT (acylated-OXT) and OXT^{Gly} (acylated-OXT^{Gly}) and demonstrated that these molecules have significantly extended half-lives *in vivo*. Compared with OXT, 2-week treatment of diet-induced obese mice with acylated-OXT [subcutaneous(ly) (SC)] resulted in enhanced body weight reduction, an improved lipid profile, and gene expression changes consistent with increased lipolysis and decreased gluconeogenesis. Treatment with acylated-OXT^{Gly} (SC) also resulted in a statistically significant weight loss, albeit to a lesser degree compared with acylated-OXT treatment. In conclusion, we demonstrate that selective activation of the OXTR pathway results in both acute and chronic metabolic benefits, whereas potential activation of vasopressin receptors by nonselective OXT analogs causes physiological stress that contributes to additional weight loss.

Freeform/Key Words: oxytocin, vasopressin, acylation, weight loss

Mammalian oxytocin (OXT) is a neuroendocrine peptide produced primarily by paraventricular and supraoptic nuclei in the hypothalamus, and it is released into circulation via the pituitary gland. The most prominent roles of OXT include parturition and milk ejection. Both of these physiological events require tissue sensitization with significant upregulation of OXT receptor (OXTR) expression in the smooth muscle of the uterus and the mammary

Abbreviations: AUC, area under the curve; DIO, diet-induced obese; EBSS, Earle's balanced salt solution; FLIPR, fluorometric imaging plate reader; GIP, gastric inhibitory peptide; GLP-1, glucagon-like peptide 1; GTT, glucose tolerance test; ICV, intracerebroventricular(ly); ipGTT, IP GTT; LC/MS, liquid chromatography/mass spectrometry; MAP, mean arterial pressure; OXT, oxytocin; OXTR, OXT receptor; SC, subcutaneous(ly); V1a, vasopressin receptor 1a; V1b, vasopressin receptor 1b; V2, vasopressin receptor 2.

Received 2 January 2019
Accepted 10 May 2019
First Published Online 16 May 2019

Research Article
July 2019 | Vol. 3, Iss. 7
doi: 10.1210/js.2019-00004 | Journal of the Endocrine Society | 1423–1444

gland, respectively [1–3]. In addition to its role in reproduction, OXT was also shown to induce psychological and behavioral changes, including enhanced maternal behaviors in female mice [4] and rats [5, 6], increased bonding behaviors in voles [7, 8], and prosocial behaviors in humans [9, 10]. As a result, OXT was tested in clinical trials for treating autism and Prader-Willi syndrome [11–15]. Owing to its analgesic and anxiolytic central effects, OXT is also being tested in clinical trials to treat pain [16, 17] and alcohol dependence and withdrawal [18–21].

More recently, OXT was found to play a critical role in metabolism and energy homeostasis. Chronic OXT treatment led to weight loss in human [22], diet-induced obese (DIO) rhesus monkey [23], and various obese rodent models [24–27]. Peripheral administration [IP or subcutaneous(ly) (SC)] of OXT suppressed food intake in DIO mice [26); central administration of OXT also led to food suppression in lean rats [28, 29] and DIO rats [30, 31]. Similarly, nasal OXT treatment reduced food or snack intake in healthy human volunteers [32-34). Interestingly, a stronger effect on food suppression was observed in subjects with obesity vs lean human subjects [35). Furthermore, clinical nasal OXT treatment suppressed hypothalamic activation to images of palatable food [36], enhanced the activities of brain regions that exert cognitive control [34], and reduced the activities of brain regions associated with both hedonic and homeostatic food motivation in human subjects [37]. Most recently, OXT, in combination with naltrexone, was shown to successfully curb hypothalamic obesity in a 13-year old male patient [38]. These anorexigenic effects of OXT are likely mediated by OXTR-expressing neurons in several brain regions, including the arcuate nucleus of the hypothalamus [39], the ventral medial nuclei of the hypothalamus [40], and brain stem neurons [25, 30, 41]. Additionally, OXT also acts on the reward circuitry, including the ventral tegmental area to regulate feeding [32, 37, 42]. In addition to its role in appetite control, OXT also plays important roles in thermoregulation [30, 43–46] and energy expenditure in rodents [40, 47, 48] and monkeys [23]. Acute OXT treatment also improved glycemic control by regulating insulin and glucagon secretion in humans and dogs [49–52]. Some studies demonstrated chronic OXT treatment-mediated improvements of glycemic control in DIO mice [26] and rats [24]. Other studies, however, demonstrated worsening of glycemic control by OXT treatment in different rodent models, including genetically obese (ob/ob) mice [53] and genetically obese Zucker rats [54]. Aside from these metabolic effects, OXT was also found to promote bone health [55] and muscle regeneration [56], reduce inflammation [57], prevent cardiomyocyte hypertrophy [58, 59], and protect against ischemia/reperfusion-induced cardiac damage [60, 61], suggesting a broad potential for the therapeutic use of OXT or OXT analogs.

Native OXT peptide lacks receptor selectivity and can activate several vasopressin receptors [62]. OXT also has an extremely short half-life of 3 to 5 minutes [62]. To understand the specific role of the OXTR pathway in metabolism, more selective and long-acting OXT peptide analogs are needed. In this study, we report the generation of a selective OXT peptide analog (OXT^{Gly}) and a selective, fatty acid–conjugated long-acting analog (acylated-OXT^{Gly}). We compared both peptides to the native OXT and its long-acting fatty acid–conjugated OXT analog (acylated-OXT) in various acute and chronic metabolic studies. We found that although native OXT (1 to 3 mg/kg, equivalent to 0.99 to 2.98 μmol/kg, IP) acutely suppressed food intake and increased mean arterial pressure (MAP), the OXTR-selective OXT^{Gly} (1 to 3 mg/kg, equivalent to 1.05 to 3.16 μmol/kg, IP) had little effect on either food consumption or MAP. Food intake suppression by OXT (2 mg/kg, equivalent to 1.98 umol/kg, IP) is abolished in the presence of vasopressin receptor 1a (V1a) and vasopressin receptor 2 (V2) inhibitor conivaptan (0.5 mg/kg, IP). Both OXT (2 mg/kg, equivalent to 1.98 μmol/kg, IP) and OXT^{Gly} (2 mg/kg, equivalent to 2.11 μmol/kg, IP) acutely stimulated insulin, glucagon, and glucagon-like peptide 1 (GLP-1) secretion *in vivo*, resulting in improved glycemic control in glucose tolerance tests (GTTs). Chronic administration of the long-acting acylated-OXT (2 μmol/kg, SC) in DIO mice resulted in significant fat and lean mass reduction, whereas chronic administration of acylated-OXT^{Gly} (2 μmol/kg, SC) caused significant fat mass reduction with no change in lean mass, thereby resulting in a moderate weight loss. Chronic treatment of

both long-acting OXT analogs led to an improved lipid profile. Taken together, our results suggest the therapeutic benefits of OXT-related peptide analogs in both acute glycemic control and chronic lipid metabolism.

1. Methods

A. Peptide Synthesis

Peptides were synthesized by solid-phase peptide synthesis using established Fmoc/tBu protocols. Specifically, an automated peptide synthesizer (Symphony, Protein Technologies, Tucson, AZ) was used. Rink amide AM was the starting resin to generate the corresponding C-terminal amide peptides, and couplings were mediated by diisopropylcarbodiimide/Oxyma in dimethylformamide with fivefold excess of reagents. For acylated-OXT and acylated-OXT^{Gly}, Lys side chain at position 8 was protected with Alloc, and after Alloc removal at the end of the peptide synthesis using $Pd(PPh_3)_4$ and phenylsilane in dichloromethane, incorporation of the linker and fatty acid in the side chain was accomplished following similar Fmoc/tBu protocols. After cleavage of the peptides from the solid support, disulfide formation for peptides OXT, acylated-OXT, and acylated-OXT^{Gly} was carried out with iodine in aqueous acetic acid conditions containing acetonitrile, excess iodine was quenched with aqueous ascorbic acid, and the solution was diluted in 0.1% trifluoroacetic acid aqueous solution. All crude peptides after cyclization were purified using reversed-phase chromatography. Purified fractions were pooled and lyophilized to generate final powder as trifluoroacetate salts. Peptides were characterized by liquid chromatography/mass spectrometry (LC/MS). The lyophilized peptides were formulated in either dimethyl sulfoxide or aqueous buffers for *in vitro* or *in vivo* testing, respectively.

B. In Vitro *Receptor Activity Assays*

For fluorometric imaging plate reader (FLIPR) calcium assays, AV12 cell clones stably expressing human OXTR, V1a, or vasopressin receptor 1b (V1b) were generated by selection against hygromycin. Cells were plated at 80,000 cells per well in 96-well, back-wall clear-bottom plates (Becton Dickinson, Franklin Lakes, NJ, catalog no. 354640) and incubated at 37°C overnight. The next day, medium was replaced with 50 μL of Fluo-4 loading buffer (Molecular Probes, Eugene, OR, catalog no. F36205), and cells were incubated for 1 hour at 37°C. Fluo-4 was then removed and replaced with Hanks balanced salt solution. Peptides with serial dilutions were prepared in Hanks balanced salt solution buffer and added to each well, and Fluo-4 fluorescent signal was read in a Tetra FLIPR machine (Molecular Devices, San Jose, CA) in real time. Concentration response curves for each peptide were generated by subtracting background fluorescence from peak fluorescence value at each peptide concentration.

For cAMP assays, HEK-293 cells were transiently transfected with a DNA construct encoding human V2 receptor. Forty-eight hours after transfection, cells were trypsinized and plated at 10,000 cells per well in half area 96-well white plate (Costar, Washington DC, catalog no. 3688) and cultured overnight. The next day, medium was removed and replaced by cAMP assay buffer (Cisbio, Bedford, MA, catalog no. 62AM4PEB). Serial dilutions of peptides were prepared in cAMP assay buffer, added to each well, and incubated with cells for 30 minutes. Cells were lysed and cAMP values were measured in an Envision plate reader (PerkinElmer, Waltham, MA) by following the manufacturer's protocol (Cisbio, catalog no. 62AM4PEB).

C. Animals and Treatments

All animal procedures were approved by the Eli Lilly Institutional Animal Care and Use Committee to ensure compliance with Federal guidelines. Male, lean C57BL/6 and male

C57BL/6 DIO mice were purchased from Taconic Biosciences (Hudson, NY) and individually housed in a controlled environment vivarium with room temperature between 22.2°C and 23.9°C on a 12-hour light/12-hour dark cycle. The mice had *ad libitum* access to water and were fed either normal chow (catalog no. 2014, Teklad, Madison, WI; Envigo, Indianapolis, IN) or a 60% high-fat diet (catalog no. D12492; Research Diets, New Brunswick, NJ). In some studies, body composition analysis was conducted on mice using quantitative nuclear magnetic resonance (EchoMRI, Houston, TX), whereby mice were placed in a clear plastic tube that was inserted into the instrument for ~1 minute or less. Body composition, including whole-body fat, lean mass, and free and total water were analyzed with MRI-based technology. Mice were euthanized via isoflurane and either serum or plasma was collected via cardiac puncture for downstream analysis.

D. Food Intake Studies

Each mouse received only one injection during the acute food intake studies. For acute food intake study, 12-week-old male C57BL/6 mice (n = 7 per group) were individually housed and fasted at the beginning of the dark cycle for 16 hours, followed by a single dose of OXT (IP) or its analogs (IP) along with immediate refeeding. The dosages for each drug are depicted in the figures and legends. The time 0 began with an initial weighing of food immediately after dosing, followed by food weighing in various increments of time, including 1, 2, 3, 4, 6, 24, and 36 hours. For the acute food intake study involving the vasopressin inhibitor conivaptan, individually housed 12-week-old male C57BL/6 mice (n = 6 per group) were dosed with vehicle or conivaptan (0.5 mg/kg, IP) at the start of the dark cycle, and food was taken away immediately after dosing. After a 16-hour fast, these mice were dosed again with conivaptan (0.5 mg/kg, IP), OXT (2 mg/kg, IP), or a combination of conivaptan (0.5 mg/kg, IP) plus OXT (2 mg/kg, IP) followed by refeeding. Food was weighed at 1, 2, and 3 hours after the second dosing. Conivaptan was dissolved in aqueous solution containing 2.5% dimethyl sulfoxide and 10% β-cyclodextrin sulfobutyl ethers (Captisol®). The same solution was used to inject animals of the vehicle control group and the OXT group.

The food intake study with central nervous system delivery of OXT and OXT^{Gly} was performed by free-hand intracerebroventricular (ICV) injection as previously described [63]. Briefly, 4-week-old male C57BL/6 mice (n = 6 per group) were individually housed and acclimated with daily handling for 5 days. At the end of fifth day, food was taken away at the start of the dark cycle. After a 16-hour fast, 3 μL of OXT (1 mg/mL), OXT^{Gly} (1 mg/mL), or vehicle was injected into the third ventricle of conscious mice by free-hand injection. Mice were put back in their home cage, and food intake was measured for 1, 2, 4, and 6 hours. The behavior of the mice was monitored for the first hour after injection, which included vocalization and scratching/grooming. Vocalization is defined by a high-pitched squeaking sound, which was only observed in OXT-injected mice but not in vehicle- or OXT^{Gly}-injected mice. Grooming is defined as self-cleaning–like behavior using the front paws, whereas scratching is defined as self-cleaning–like behavior using the hind paws. Injection site accuracy was verified by *post hoc* examination of the brain. Because the free-hand ICV drug delivery does not involve anesthetics, mouse behaviors can be monitored immediately after the injection.

E. Chronic OXT Analog Treatment in DIO Mice

Twenty-week-old DIO mice (n = 7 per group) were fed with a high-fat diet (Research Diets, catalog no. D12492) beginning at 4 weeks of age and were individually housed. OXT (2 μmol/kg), acylated-OXT (2 μmol/kg), and acylated-OXT^{Gly} (2 μmol/kg) were injected (SC) once daily. The study began with an initial 16-hour fast, followed the next morning by dosing of OXT analogs and immediate refeeding and weighing food. The mice were dosed (SC) daily, and food and body weight were successively measured thereafter, daily, for the duration of the study.

F. GTTs

Individually housed C57BL/6 lean mice (n = 6 per group) or DIO mice (n = 6 per group) were fasted for 4 hours prior to the start of GTTs. Thirty minutes prior to dextrose injection, the mice were IP injected with OXT (2 mg/kg) or OXT^{Gly} (2 mg/kg). Thirty minutes later, the mice received IP injections of 1 or 2 mg/kg dextrose (Hospira, Lake Forest, IL), and subsequent blood glucose was measured by AccuCheck Aviva standard blood glucose monitors (Roche Diagnostics, Indianapolis, IN) from blood samples collected via venipuncture of the tail vein at baseline and 15, 30, 60, and 120 minute time points.

G. Pharmacokinetic Measurement by Mass Spectrometry

For pharmacokinetic studies, 11-week-old C57BL/6 mice (n = 3 per group) received a single injection (1 mg/kg, IP) of OXT analogs (either OXT, OXT^{Gly}, acylated-OXT, or acylated-OXT^{Gly}). Plasma was collected via cardiac puncture at 0.5, 1, 3, 6, and 24 hours postinjection. Plasma samples were stored at −80°C until analysis.

Formic acid was added to 50 μL of mouse plasma sample to a final concentration of 4%. Peptides were then extracted from the acidified plasma using 3 volumes (150 μL) of acetonitrile, followed by a 2-hour incubation on ice. Extraction supernatants were dried under nitrogen gas, and the resulting pellets were resuspended with 150 μL of 0.1% formic acid in water. These samples were subjected to LC/MS analysis using a Shimadzu LC-30AD and a Sciex 6500+ triple quadrupole mass spectrometer. Chromatographic separation was achieved using a Waters XBridge C18 (2.1 × 50 mm, 3.5 μm) analytical column held at 40°C. Mobile phase A was 0.1% formic acid in water and mobile phase B was 0.1% formic acid in acetonitrile. Using a flow rate of 0.6 mL/min, mobile phase B was held at 2% for 0.5 minutes followed by a 15% to 95% ramp for 3.3 minutes. Mobile phase B was then held at 95% for 1.2 minutes before returning to 2% for reequilibration. Mass spectra were collected in the scheduled multiple reaction monitoring mode with positive polarity and unit resolution. For each OXT analog, the parent→b6 transition was primarily monitored. The resulting data were analyzed using the Sciex MultiQuant 3.0.2 software.

Standard curves for each OXT analog were generated using a mouse plasma pool spiked with synthetic OXT peptide analogs and the above extraction and LC/MS detection methodologies.

H. Rat Blood Pressure Telemetry

DIO male Long-Evans rats (Envigo) were maintained on a calorie-rich diet (catalog no. TD95217; Teklad) since weaning. The rats were individually housed in a temperature-controlled (24°C) facility with a 12-hour light/12-hour dark cycle. Surgery was performed to implant the blood pressure transmitter when the rats were 15 weeks old. Briefly, rats were anesthetized with 3% isoflurane. Under aseptic conditions, a 2- to 3-cm incision was made at the inner thigh above the left femoral triangle, and the femoral artery was isolated. A mid-abdominal incision was carried out and the electric transmitter (model TA11PA-C40; Data Sciences International, St. Paul, MN) was sutured to the inside of abdominal muscles. The catheter of the transmitter was punched and passed through the abdomen into the left femoral triangle using a 14-gauge, 1.5-inch syringe needle as a trocar, followed by insertion into the femoral artery up to about 5 cm until reaching the position of the renal arteries. The transmitter was fixed within the peritoneal cavity by suturing to the abdominal muscles. The proximal suture was tied around the vessel and catheter, and the distal suture was tied around the catheter to secure. Both incisions were closed, and the rats were allowed to recover from surgery for 2 weeks and then were placed in individual cages.

The animals (n = 6 per group) were 40 weeks of age when the blood pressure study was performed. Various doses (0.3 mg/kg, 1 mg/kg, 3 mg/kg) of OXT and OXT^{Gly} were IP injected following an escalating dose design. Briefly, each rat from the OXT and the OXT^{Gly} groups received a low dose (0.3 mg/kg), a medium dose (1 mg/kg), and a high dose (3 mg/kg), with

24 hours of recovery time between each dose, whereas blood pressure and food intake were monitored continuously in real time throughout the experiment. Digitized pressure signals were acquired for 30 seconds every 5 minutes using DSI Dataquest IV 4.0 software.

I. Acute Incretin and Hormone Measurements in Mice

Sixteen-week-old C57BL/6 male (n = 5 per group per time point) were individually housed and fasted for 16 hours at the start of dark cycle. The next day, animals were IP injected with OXT (2 mg/kg) or its analog OXT^{Gly} (2 mg/kg) and placed back into their home cage without food. At given time points (15, 30, 60, and 180 minutes) after injection, the groups of animals were euthanized and their plasma was collected by cardiac puncture. Plasma concentrations of insulin, glucagon, GLP-1, and gastric inhibitory peptide (GIP) were measured as described below.

J. Biochemical Assays

Glucagon (catalog no. K150HCC) [64] and total GLP-1 (catalog no. K150JVC) [65] were assayed using Meso Scale Discovery (Rockville, MD) multi-array system kits. Active GIP was measured in plasma via rat/mouse GIP (total) ELISA (catalog no. EZRMGIP-55K; Millipore, Burlington, MA) [66]. Briefly, plasma EDTA tubes (catalog no. 365974; BD Biosciences, Franklin Lakes, NJ) were kept at 4°C or on ice and pretreated with aprotinin (catalog no. BP2503; Fisher Scientific, Hampton, NH) and dipeptidyl peptidase IV inhibitor (catalog no. DPP4-010; Fisher Scientific) to prevent natural breakdown of GLP-1 and GIP. Plasma was collected via cardiac puncture into microtainer tubes, centrifuged for 20 minutes at 2000 rpm at 4°C, and analyzed using the above-mentioned kits by following the manufacturers' protocols. Insulin was measured using an in-house assay based on the MSD platform. In some studies, serum was collected in SST tubes (catalog no. 365967; BD Biosciences) and submitted to our in-house Clinical Pathology Group for a clinical chemistry panel performed on the Roche Hitachi P modular chemistry analyzer. Specifically, creatinine was examined via enzymatic method and blood triglycerides were glycerol banked. Liver triglycerides were measured in a Hitachi Cobas instrument. Briefly, livers that had been previously flash-frozen and stored at −80°C were weighed and used to prepare a 20% homogenate in deionized water on the FastPrep-24 (MP Biomedicals, Santa Ana, CA). The samples were diluted 1:4 in at least 75 μL of water and run as "supernatant" on the instrument.

K. Insulin and Glucagon Secretion by Primary Mouse and Human Islets

Mouse pancreatic islets were isolated from male C57BL/6 mice (27 to 30 g, Harlan Laboratories, Indianapolis, IN) by collagenase digestion. Human pancreatic islets were purchased from Prodo Laboratories (Irvine, CA) and InSphero (Schlieren, Switzerland) and obtained from human pancreata from listed cadaver organ donors that were refused for primary human pancreas transplantation or from isolated islets transplanted into listed recipients with diabetes.

Islets were cultured in RPMI 1640 medium (Life Technologies, Grand Island, NY) supplemented with 10% heat-inactivated fetal bovine serum (Life Technologies), 100 IU/mL penicillin, and 100 μg/mL streptomycin (Life Technologies). Insulin secretion in mouse and human pancreatic islets was measured as follows: islets were incubated for 30 minutes in Earle's balanced salt solution (EBSS) buffer supplemented with 3 mM glucose and 0.1% BSA. Then groups of three islets were selected and cultured with peptides in 300 μL of EBSS for 60 minutes at 37°C. At the end of incubation, the supernatant was collected and subjected to insulin analysis. To measure insulin and glucagon secretion in human pancreatic islets from InSphero, single islets placed in a GravityTRAP 96-well plate (InSphero) were washed and incubated for 30 minutes in 100 μL of EBSS supplemented with 0.1% BSA and 5 mM glucose. Then the buffer was replaced with 100 μL of EBSS containing indicated

glucose and peptide concentrations and further cultured for 60 minutes at 37°C. At the end of incubation, the supernatant was collected and submitted for insulin and glucagon analysis as mentioned above.

L. Real-Time RT-PCR

Tissues, including liver and fat, were obtained at the end of the study, snap frozen in liquid nitrogen, and subsequently stored at −80°C. RNA was isolated from frozen tissues using TRIzol reagent (catalog no. 15596018; Thermo Fisher Scientific, Waltham, MA) according to the manufacturer's protocol. Briefly, the tissues were homogenized in TRIzol using FastPrep-24. 1-Bromo-3-chloropropane (catalog no. BP 151; Molecular Research Center, Cincinnati, OH) was added for phase separation, after which the aqueous layer containing RNA was removed into a deep-well plate. The RNA was ethanol precipitated, purified using the a PerfectPure RNA 96 cell kit (5 Prime, Hamburg, Germany), and quantified using a NanoDrop 8000 (Thermo Scientific). Five hundred nanograms to 2 μg (tissue-dependent) of cDNA was generated using a high-capacity reverse transcription kit (catalog no. 43368814; Thermo Fisher Scientific) according to the manufacturer's protocol. RT-PCR was performed using mouse TaqMan (Applied Biosystems, Foster City, CA) hydrolysis probes, Fast Advanced Master Mix (catalog no. 444965; Applied Biosystems), and the ABI QuantStudio 7 Flex real-time PCR system (Thermo Fisher Scientific). Results were tissue-dependently normalized to the housekeeping genes 18S, RPLP0, or hypoxanthine phosphoribosyltransferase.

M. Statistical Analysis

Statistical analysis was performed using GraphPad Prism (GraphPad Software, La Jolla, CA). Values were obtained using either two-way ANOVA or one-way ANOVA with Dunnett multiple comparisons. Values are expressed as the mean ± SEM, and significance was established at $P < 0.05$.

2. Results

A. Receptor Selective OXT Peptide Analogs

To identify OXT peptide analogs that are specific to OXTR, we first replaced the cysteine at position 1 with a butyryl N-terminal capping group that forms a covalent thioether bond with the side chain of cysteine at position 6 ($OXT^{Butyryl}$). $OXT^{Butyryl}$ also contains *O*-methylated tyrosine at position 2 and has the same chemical structure as carbetocin, a US Food and Drug Administration–approved OXT analog. We found that this N-terminal modification resulted in increased receptor selectivity against vasopressin receptors without affecting OXTR activation [67]. Next, we replaced proline at position 7 with glycine on $OXT^{Butyryl}$ and named this new peptide analog OXT^{Gly} [67]. We then tested OXT^{Gly} selectivity against the OXTR, and V1a and V1b using a FLIPR calcium assay, and V2 using cAMP assays. As shown in Fig. 1, OXT^{Gly} is highly selective against V1a, V1b, and V2, and it retained similar OXTR activity compared with OXT. When compared with a small-molecule OXTR-specific agonist (WAY-267464), OXT^{Gly} showed similar OXTR selectivity and superior OXTR potency [67]. Therefore, OXT^{Gly} is a potent and selective peptide ligand for OXTR.

B. OXT^{Gly} Functions as a Highly Selective OXTR Agonist In Vivo

A known physiological action of vasopressin is vasoconstriction leading to increased blood pressure [68]. Because native OXT partially activates vasopressin receptors whereas OXT^{Gly} does not, we tested whether treatment with these peptides would differentially affect blood pressure. Consistent with previous reports [69], OXT (IP) dose-dependently caused a

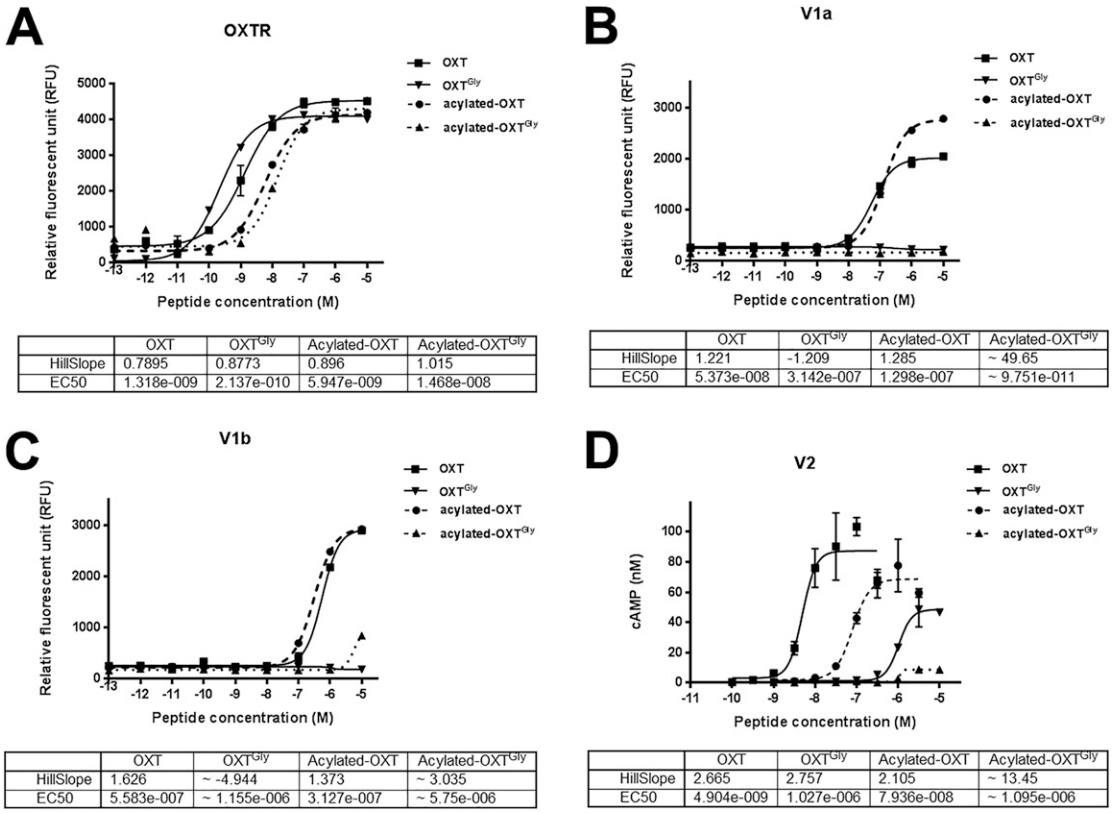

	OXT	OXT^{Gly}	Acylated-OXT	Acylated-OXT^{Gly}
HillSlope	0.7895	0.8773	0.896	1.015
EC50	1.318e-009	2.137e-010	5.947e-009	1.468e-008

	OXT	OXT^{Gly}	Acylated-OXT	Acylated-OXT^{Gly}
HillSlope	1.221	-1.209	1.285	~ 49.65
EC50	5.373e-008	3.142e-007	1.298e-007	~ 9.751e-011

	OXT	OXT^{Gly}	Acylated-OXT	Acylated-OXT^{Gly}
HillSlope	1.626	~ -4.944	1.373	~ 3.035
EC50	5.583e-007	~ 1.155e-006	3.127e-007	~ 5.75e-006

	OXT	OXT^{Gly}	Acylated-OXT	Acylated-OXT^{Gly}
HillSlope	2.665	2.757	2.105	~ 13.45
EC50	4.904e-009	1.027e-006	7.936e-008	~ 1.095e-006

Figure 1. Receptor selectivity of OXT peptide analogs. (A) FLIPR assay of AV12 cells stably expressing human OXTR. (B) FLIPR assay of AV12 cells stably expressing hV1a. (C) FLIPR assay of AV12 cells stably expressing hV1b. (D) cAMP assay of HEK-293 cells transiently expressing hV2.

statistically significant increase of MAP in DIO Long-Evans rats [67]. In contrast, OXT^{Gly} (IP) did not result in detectable MAP increase over baseline at any dose tested [67]. Together with receptor selectivity assays (Fig. 1), these results suggest that OXT^{Gly} functions as a selective OXTR agonist both *in vitro* and *in vivo*.

C. Generation of Nonselective and Selective Long-Acting OXT Peptide Analogs Using Fatty Acid Modification (Acylation) as a Time Extension Strategy

Next, we sought to extend the half-life of OXT peptides by covalently attaching a fatty acid moiety to the peptide backbone. Fatty acids act as noncovalent albumin-binding motifs resulting in extended peptide pharmacokinetics. We performed a peptide backbone scan to replace each amino acid in the OXT sequence with a lysine-$(AEEA)_2$-$(\gamma E)_2$-C18 dicarboxylic acid moiety including the N-terminal (position 0) and C-terminal extended sequence (position 10), with the exception of the two cysteine residues. The analog with a lysine-$(AEEA)_2$-$(\gamma E)_2$-C18 dicarboxylic acid moiety replacing the leucine at position 8 was the most potent out of this series at the OXTR and had a similar selectivity profile to native OXT (Fig. 1 and data not shown). This peptide analog was named acylated-OXT [67]. Consequently, we replaced proline at position 7 in the acylated-OXT with glycine to generate the acylated-OXT^{Gly} analog [67] and showed that it retained similar OXTR activity compared with acylated-OXT (Fig. 1A), and that it was highly selective for the OXTR relative to V1a, V1b, and V2 (Fig. 1B–1D). Therefore, we successfully generated potent nonselective and selective acylated-OXT analogs for *in vivo* evaluation.

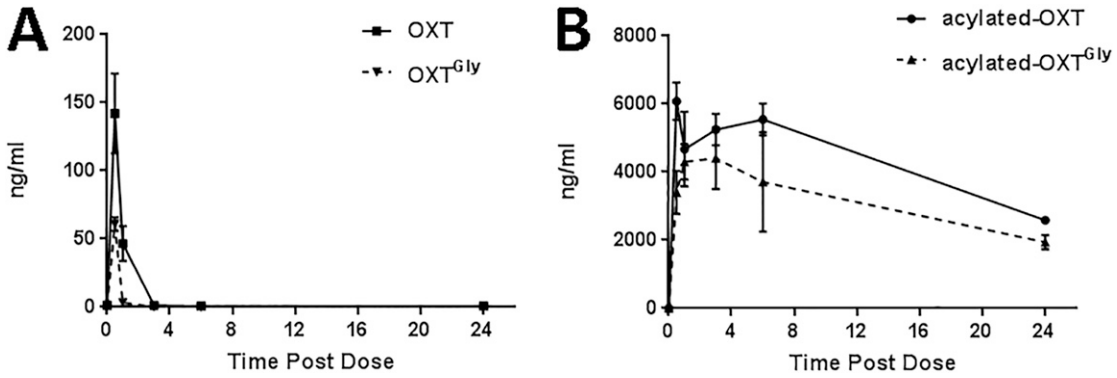

Figure 2. Pharmacokinetics of OXT peptide analogs in mice. (A and B) Sixteen-wk-old naive male C57BL/6 mice (n = 3 per group) received a single dose (1 mg/kg, IP) of OXT or OXT^{Gly} (A) or acylated-OXT or acylated-OXT^{Gly} (B). Plasma was collected at 0.5, 1, 3, 6, and 24 h after dosing via cardiac puncture. Circulating levels of each peptide were quantified by mass spectrometry analysis.

D. Pharmacokinetics of OXT Peptide Analogs

We measured the pharmacokinetics of OXT, OXT^{Gly}, acylated-OXT, and acylated –OXT^{Gly} using mass spectrometry. When IP injected into C57BL/6 mice, OXT and OXT^{Gly} had similar short pharmacokinetics profiles. Plasma levels of OXT and OXT^{Gly} peaked at around 30 minutes after injection and dropped quickly to below detection in <3 hours (Fig. 2A). This result is consistent with numerous reports that OXT peptide has a very short half-life ranging from a few minutes in humans [70] and rats [71] to 10s of minutes in monkeys [72], and it suggests that neither the butyryl substitution at the N terminus nor the glycine substitution at position 7 led to half-life extension *in vivo*. In contrast, the acylated-OXT and acylated-OXT^{Gly} had significantly prolonged exposure *in vivo*. The plasma levels of these two long-acting peptide analogs peaked between 1 and 4 hours postinjection and remained >50% of the peak concentration at 24 hours after the initial dose (Fig. 2B). Both OXT and OXT^{Gly} yielded significantly lower levels of detection in plasma compared with acylated peptides (Fig. 2A vs Fig. 2B), which is consistent with their extremely short half-lives being less than the first detection time point of 30 minutes. In summary, fatty acid conjugation significantly extended the half-life of OXT peptides *in vivo*.

E. Dynamic and Differential Effects of OXT Analogs on Food Consumption

Next, we tested the effect of OXT peptide analogs on food intake in lean C57BL/6 mice. Consistent with previous reports, OXT (IP) dose-dependently suppressed food intake in 16-hour fasted animals (Fig. 3A). A high dose (2 mg/kg, equivalent to 1.98 μmol/kg, IP) of OXT led to reduction in food intake for up to 24 hours, but not at 36 hours postinjection (Fig. 3B). In contrast, a medium (1 mg/kg, equivalent to 0.54 μmol/kg, IP) or high (4 mg/kg, equivalent to 2.14 μmol/kg, IP) dose of acylated-OXT significantly suppressed food consumption for >24 hours in a dose-dependent manner (Fig. 3B). The sustained food suppression effect by acylated-OXT is consistent with its pharmacokinetic property *in vivo* (Fig. 2B).

To examine whether an OXTR-selective agonist would similarly inhibit food intake, we tested the effect of OXT^{Gly} on food consumption. As shown in Fig. 3C, IP administration of OXT^{Gly} at various dosages did not cause a statistically significant reduction in food intake during the first 3 hours postinjection (Fig. 3C). We further compared the effects of high-dose OXT vs OXT^{Gly} side by side in a 24-hour food intake study. As shown in Fig. 3D, OXT (2 mg/kg, equivalent to 1.98 μmol/kg, IP), but not OXT^{Gly} (2 mg/kg, equivalent to 2.11 μmol/kg, IP), caused a significant reduction in food intake for the first 6 hours postinjection. Cumulative food consumption in the OXT^{Gly}-treated group trended lower compared with the vehicle group and reached statistical significance at 24 hours after treatment (Fig. 3D). To exclude

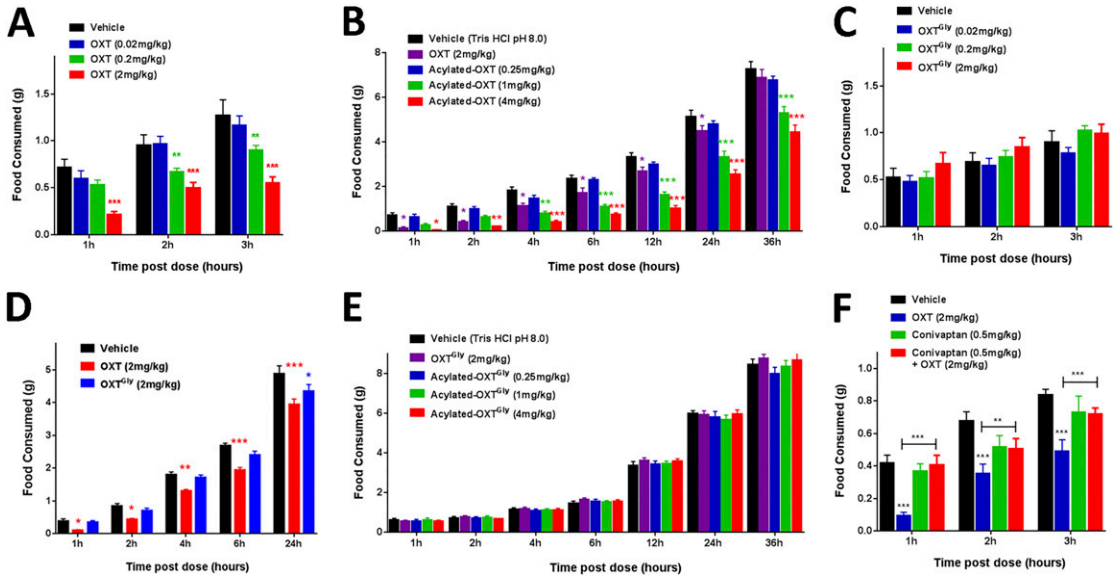

Figure 3. Food intake suppression by OXT analogs is modulated by their pharmacokinetic properties and receptor selectivity. (A) A single injection (IP) of OXT dose-dependently suppressed food intake in lean male C57BL/6 mice (n = 7 per group) for up to 3 h. (B) A single injection (IP) of acylated-OXT dose-dependently suppressed food intake in lean male C57BL/6 mice (n = 7 per group) for up to 36 h. (C) Various doses of OXT^{Gly} (IP) did not cause reduction in food intake in lean male C57BL/6 mice (n = 7 per group). (D) Twenty-four hour food intake measurement after a single injection (IP) of OXT (2 mg/kg) or OXT^{Gly} (2 mg/kg) in lean male C57BL/6 mice (n = 7 per group). (E) Various doses of acylated-OXT^{Gly} (IP) did not cause food intake reduction in lean male C57BL/6 mice (n = 7 per group). (F) Food intake after coinjections (IP) of conivaptan (0.5 mg/kg) and OXT (2 mg/kg) in lean male C57BL/6 mice (n = 6 per group). For OXT, 1 mg/kg = 0.99 μmol/kg; for OXT^{Gly}, 1 mg/kg = 1.05 μmol/kg; for acylated-OXT, 1 mg/kg = 0.54 μmol/kg; for acylated-OXT^{Gly}, 1 mg/kg = 0.55 μmol/kg. $*P < 0.05$, $**P < 0.01$, $***P < 0.001$, two-way ANOVA followed by a Tukey multiple comparisons test.

the possibility that the lack of an effect of OXT^{Gly} is due to its inability to access brain regions responsible for food intake regulation, we directly injected OXT^{Gly} into the central nervous system via ICV injection and measured its effect on food intake in 4-week-old 16-hour fasted male C57BL/6 mice. Whereas OXT (3 μg per mouse, ICV) acutely suppressed food consumption at 1 hour after dosing, OXT^{Gly} (3 μg per mouse, ICV) did not produce any effect on food consumption at all the time points measured [67]. Finally, we tested whether the long-acting acylated-OXT^{Gly} affected food intake. As shown in Fig. 3E, treatment with various doses of acylated-OXT^{Gly} (IP) did not affect food intake in 16-hour fasted mice. Consistent with these data in mice, we also found that OXT (IP), but not OXT^{Gly} (IP), treatment dose-dependently led to reduced food intake in DIO rats [67]. Taken together, these results suggest that the acute food intake suppression observed following OXT administration is mediated, at least in part, via activation of vasopressin receptors.

To further test this hypothesis, we conducted a food intake study in the presence of a US Food and Drug Administration–approved vasopressin receptor blocker, conivaptan, which inhibits both V1a and V2 [73]. Consistent with our hypothesis, conivaptan (0.5 mg/kg, IP, see *Methods* for details) coadministered with OXT (2 mg/kg, IP) abolished OXT's effect on food intake suppression (Fig. 3F).

F. OXT Analogs Improve Glycemic Control in Lean and Obese Mice

To test whether OXT analogs affect blood glucose regulation, we conducted an IP GTT (ipGTT) in lean C57BL/6 mice. Both OXT (2 mg/kg, IP) and OXT^{Gly} (2 mg/kg, IP) treatments

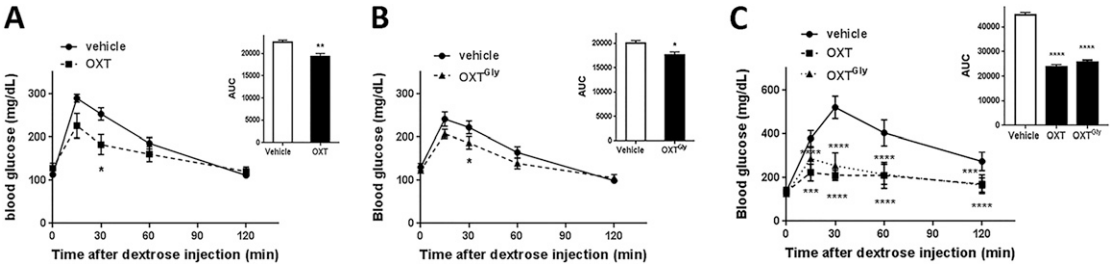

Figure 4. OXT and OXT^{Gly} treatment improved glycemic control in lean and obese animals. (A) Effect of OXT (2 mg/kg, IP) on ipGTT in lean 16-wk-old C57BL/6 mice (n = 6 per group). (B) Effect of OXT^{Gly} (2 mg/kg, IP) on ipGTT in lean 16-wk-old C57BL/6 mice (n = 6 per group). (C) ipGTT study comparing OXT (2 mg/kg, IP) vs OXT^{Gly} (2 mg/kg, IP) in 16-wk-old DIO C57BL/6 mice (n = 6 per group). The curves were analyzed using two-way ANOVA followed by a Dunnett multiple comparisons test. An unpaired *t* test was used to analyze the AUC in panels (A) and (B); a one-way ANOVA followed by a Dunnett multiple comparisons test was used to analyze the AUC in panel (C). For all analyses: $*P < 0.05$, $**P < 0.01$, $***P < 0.001$, $****P < 0.0001$.

led to moderate yet statistically significant reductions of blood glucose (Fig. 4A and 4B). The blood glucose, as measured by the area under the curve (AUC), was reduced by 14.5% ± 8% and 11.7% ± 7% for OXT and OXT^{Gly} treatments, respectively, when compared with vehicle treatment (Fig. 4A and 4B). We subsequently tested these OXT analogs in DIO mice and found that administration of either OXT (2 mg/kg, IP) or OXT^{Gly} (2 mg/kg, IP) led to a much greater reduction in blood glucose in the ipGTT. Blood glucose AUC was reduced by 47.2% ± 5.5% and 42.8% ± 4.8% for OXT and OXT^{Gly} treatments, respectively, when compared with vehicle treatment (Fig. 4C).

G. OXT Analogs Stimulate Secretion of Endocrine Hormones and Incretins

To understand how OXT analogs regulate blood glucose, we measured levels of circulating hormones after OXT analog injection into C57BL/6 mice. As shown in Fig. 5, administration of both OXT (2 mg/kg, IP) and OXT^{Gly} (2 mg/kg, IP) led to rapid increases in circulating levels of insulin (Fig. 5A and 5A′), glucagon (Fig. 5B and 5B′), and GLP-1 (Fig. 5C and 5C′). The level of active GIP was not affected by either OXT or OXT^{Gly} administrations (Fig. 5D and 5D′).

Furthermore, we asked whether OXT analogs directly regulate insulin secretion. We treated mouse primary islets with OXT and OXT^{Gly} and measured insulin secretion. Both OXT and OXT^{Gly} dose-dependently stimulated insulin secretion from isolated mouse primary islets (Fig. 6A). Surprisingly, neither OXT nor OXT^{Gly} stimulated insulin secretion in isolated human islets (Fig. 6B). We also examined whether OXT analogs affect glucagon secretion in these islets. Incubation of human islets in the presence of low glucose (3 mM) increased glucagon secretion relative to high-glucose (11 mM) medium (Fig. 6C). In the presence of high glucose, OXT^{Gly} significantly increased glucagon secretion compared with the high-glucose control–treated islets (Fig. 6C), suggesting that the OXT pathway directly stimulates human α-cells to secrete glucagon.

H. OXT Analogs Promote Weight Loss in Obese Mice

Native OXT peptide treatments were previously shown to cause weight loss in rodents [22, 24, 26, 30, 31, 74], monkeys [23], and humans [22]. We hypothesized that long-acting OXT analogs would result in a more substantial effect on body weight reduction, compared with native OXT, due to their superior pharmacokinetics. To test this, we chronically treated DIO mice with long-acting OXT analogs and compared their effects to native OXT peptide treatment. As shown in Fig. 7A, daily injection of OXT (2 μmol/kg, SC) led to a significant body weight reduction (−5.8% ± 0.7%) compared with vehicle treatment during a 14-day

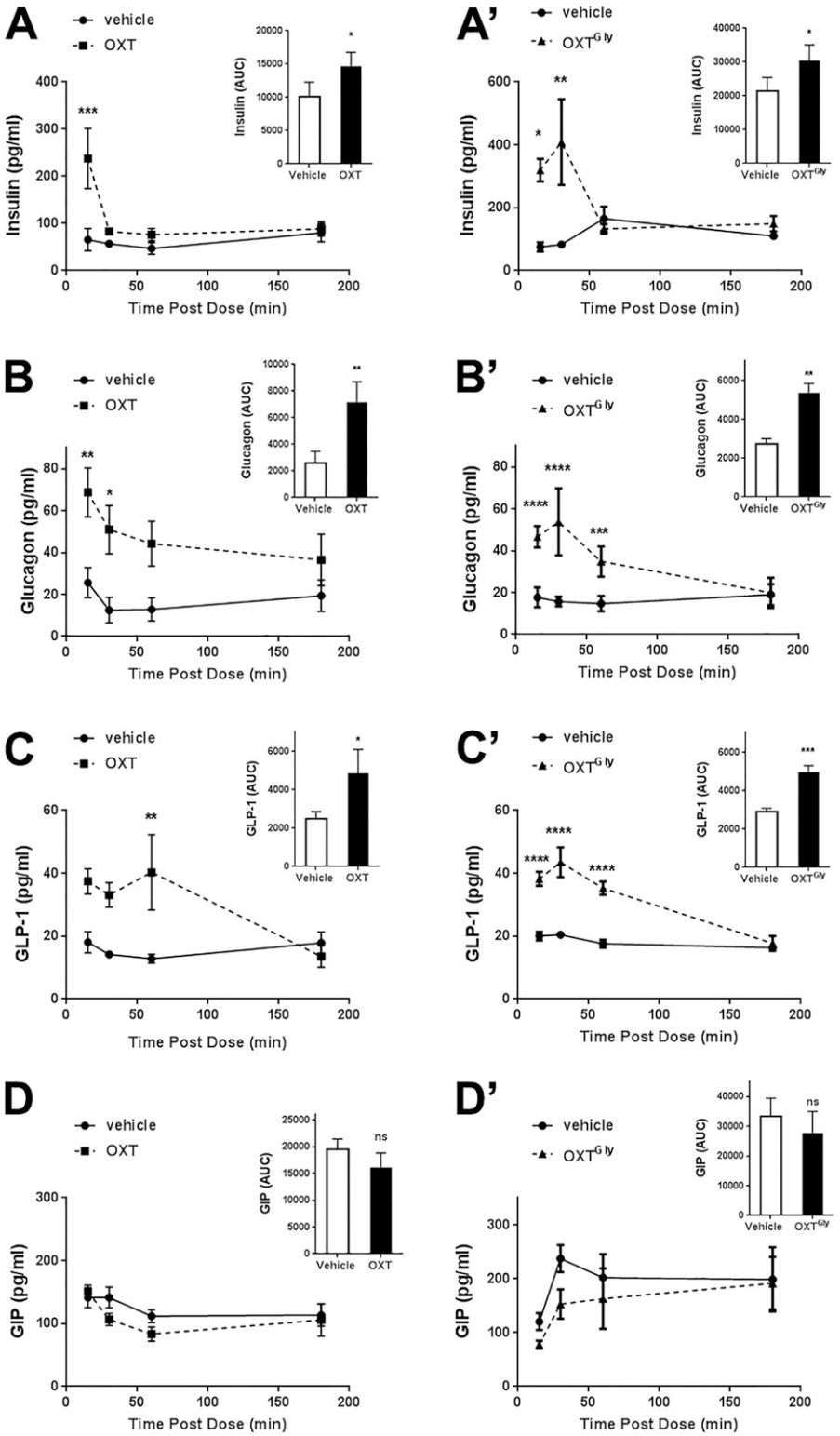

Figure 5. OXT stimulates insulin, glucagon, and GLP-1 secretion. OXT (2 mg/kg) (A–D) and OXT^{Gly} (2 mg/kg) (A′–D′) were IP injected into 16-wk-old C57BL/6 mice (n = 5 per group per time point) 30 min prior to the first blood hormone measurements. Mice were killed at given time points, and circulating hormones including insulin (A and A′), glucagon (B and B′), GLP-1 (C and C′), and active GIP (D and D′) were measured. $^{*}P < 0.05$, $^{**}P < 0.01$, $^{***}P < 0.001$, $^{****}P < 0.0001$, two-way ANOVA followed by a Dunnett multiple comparisons test. An unpaired t test was used to analyze the AUC.

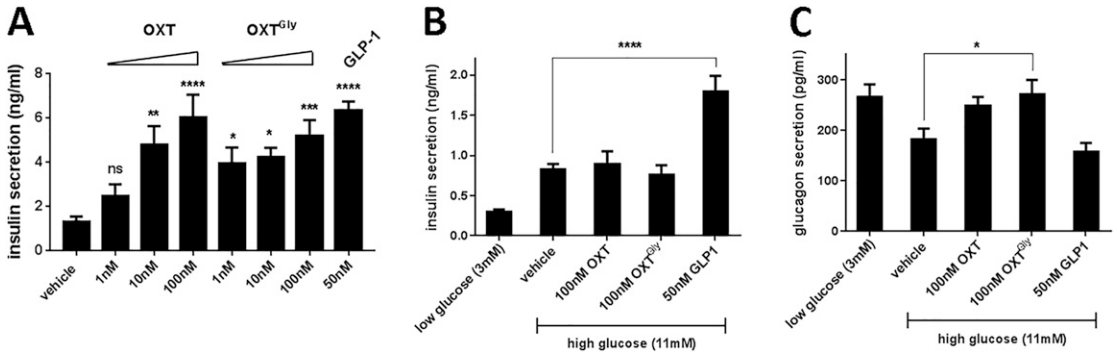

Figure 6. OXT and OXT^{Gly} directly stimulate insulin and glucagon secretion from primary islets. (A) Isolated mouse islets were treated with OXT and OXT^{Gly} for 2 h in the presence of 11 mM glucose. OXT and OXT^{Gly} dose-dependently increased insulin secretion into culture medium compared with vehicle treatment. (B) Isolated human islets were treated with OXT and OXT^{Gly} for 2 h in the presence of 3 mM or 11 mM glucose. Insulin secreted into culture supernatant was quantified. (C) Isolated human islets treated with OXT and OXT^{Gly} for 2 h in the presence of either 3 mM glucose as control or 11 mM glucose. Glucagon secreted into culture supernatant was quantified. *$P < 0.05$, **$P < 0.01$, ***$P < 0.001$, ****$P < 0.0001$, one-way ANOVA followed by a Dunnett multiple comparisons test against the vehicle control group.

treatment. Consistent with our hypothesis, acylated-OXT treatment (2 μmol/kg, SC) led to a significantly greater (−13.2% ± 0.7%) weight loss (Fig. 7A). Treatment with acylated-OXT^{Gly} (2 μmol/kg, SC) also led to a significant (−6.7% ± 1.7%) weight loss compared with vehicle treatment that was similar to that observed with OXT treatment (Fig. 7A). Interestingly, the weight loss effect by acylated-OXT appeared as early as 1 day after initial injection and plateaued after 4 days of injection (Fig. 7A), whereas acylated-OXT^{Gly} treatment induced a gradual reduction in body weight with sustained and statistically significant weight loss after 9 days of treatment (Fig. 7A).

Similar to its effect on acute food suppression, chronic treatment with acylated-OXT (2 μmol/kg, SC) suppressed food intake by 21%, resulting in 27.0 ± 1.0 g of total food consumption during the 14-day treatment compared with 34.3 ± 0.9 g of food consumption in the vehicle group (Fig. 7B). Although acute OXT^{Gly} (IP) treatment had a very modest effect on food consumption (see Fig. 3C and 3D), chronic treatment with acylated-OXT^{Gly} (2 μmol/kg, SC) suppressed food consumption by 14% and resulted in 29.4 ± 1.6 g of cumulative food intake, compared with vehicle, at the end of the study (Fig. 7B). Consistent with the observed weight loss, acylated-OXT and acylated-OXT^{Gly} caused significant fat mass reduction in DIO mice (Fig. 7C). Intriguingly, acylated-OXT^{Gly} treatment, but not OXT or acylated-OXT treatments, preserved lean mass (Fig. 7C), suggesting differential effects on lean mass metabolism between receptor-selective and nonselective OXT analogs.

The reduction of fat mass in OXT analog–treated mice was accompanied with significantly decreased plasma low-density lipoprotein cholesterol (Fig. 7D), liver triglycerides (Fig. 7E), and a trend toward lower plasma free fatty acid (Fig. 7F). Furthermore, changes in gene expression in the liver are consistent with weight loss and improved fat metabolism. Expression of FGF21, a metabolic hormone, was significantly increased in both the acylated-OXT– and the acylated-OXT^{Gly}–treated groups (Fig. 7G). Expression of the gluconeogenesis gene G6Pase was significantly decreased, whereas the expression of genes regulating glycolysis, PepCK and GCK, did not show significant changes in DIO mouse liver (Fig. 7G).

Finally, we conducted an ipGTT at the end of the 14-day treatment. To our surprise, none of the OXT analogs led to improvement of glycemic control after chronic treatment (Fig. 7H). On the contrary, acylated-OXT and acylated-OXT^{Gly} showed a modest increase in glucose level at the 60-minute time point during the GTT, and trended higher when measured as the glucose AUC (Fig. 7H and 7I). Additionally, fasting glucose trended higher in the acylated-OXT– and the acylated-OXT^{Gly}–treated groups compared with the vehicle group (Fig. 7J). Circulating

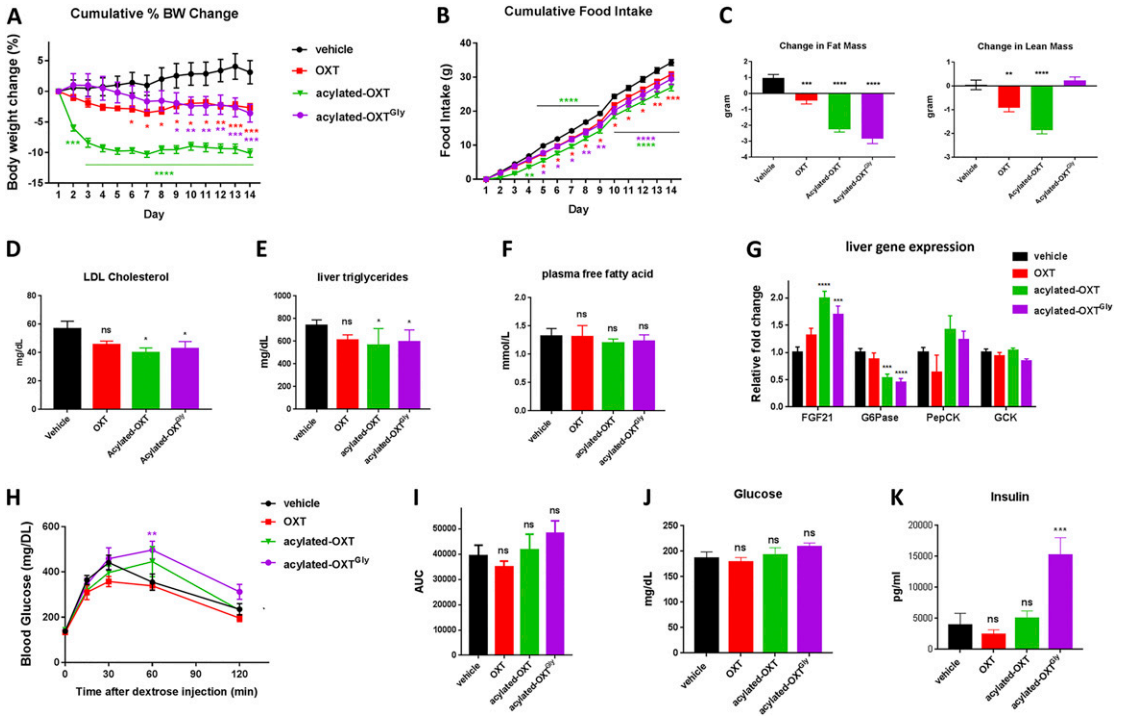

Figure 7. Long-acting acylated-OXT and acylated-OXT^{Gly} promote weight loss and lipid metabolism *in vivo*. Twenty-week-old C57BL/6 DIO mice (n = 7 per group) were dosed daily with OXT analogs (2 μmol/kg, SC) for 2 wk. (A) Cumulative body weight change. (B) Cumulative food consumption. (C) Fat and lean mass were measured by quantitative nuclear magnetic resonance at the beginning and end of study. (D–F) Plasma low-density lipoprotein (LDL) cholesterol (D), liver triglyceride (E), and plasma free fatty acid (F) were measured at the end of the study. (G) Liver gene expression changes. (H and I) ipGTTs were conducted at the end of the study. (J and K) Fasting plasma glucose (J) and insulin (K) were also measured at the end of study. Two-way ANOVA followed by a Dunnett multiple comparisons test were used for (A), (B), and (H). One-way ANOVA followed by a Dunnett multiple comparisons test were used for panels (C)–(G) and (I)–(K). For all statistical analyses: * $P <$ 0.05, ** $P < 0.01$, *** $P < 0.001$, **** $P < 0.0001$.

insulin was significantly higher in mice treated with acylated-OXT^{Gly} compared with all other treatment groups (Fig. 7K).

Because vasopressin is known to regulate osmotic balance by modulating kidney function, we monitored serum electrolytes and biomarkers for kidney function. We found that serum potassium levels were significantly lower in OXT-treated mice, and even more so in acylated-OXT–treated mice, compared with vehicle treatment [67]. In contrast, receptor-selective acylated-OXT^{Gly} treatment did not cause a statistically significant potassium decrease [67]. Because V2 agonists are known to induce kaliuresis, leading to a reduced serum potassium level [75, 76], our results suggest that OXT and acylated-OXT activated V2 *in vivo*, whereas acylated-OXT^{Gly} is specific to OXTR and did not stimulate V2-mediated kaliuresis. Sodium was not affected in any of the treatment groups, whereas calcium and chloride were modestly affected [67]. Kidney function appeared normal in all treatment groups as indicated by normal blood urea nitrogen and creatinine levels [67].

3. Discussion

To date, most metabolic studies of OXT have been performed using the native OXT peptide, which has a very short half-life and activates vasopressin receptors to various extents. These properties limit the effectiveness of OXT and confound studies intended to ascertain the specific physiological role of the OXTR. To overcome these issues, we synthesized OXT

analogs and identified those with a high degree of OXTR selectivity and those with both improved selectivity and pharmacokinetic properties. When tested *in vivo*, these novel OXTR-selective analogs showed a significant beneficial effect on acute glycemic control, whereas chronic dosing of these analogs caused weight loss and improved lipid metabolism without significant benefit in glycemic control. Our results unambiguously demonstrated the metabolic benefits of targeting the OXTR pathway.

OXT and vasopressin are both 9–amino acid peptides with an intrachain disulfide bond. They differ from each other at only two amino acid positions. OXT is 5- to 100-fold selective toward its native receptor compared with vasopressin receptors (V1a, V1b, and V2) (Fig. 1) [62]. A few peptide analogs, most notably (Thr4, Gly7)-OXT (commonly referred to as TGOT) and carba-1-(4-FBzlGly7)dOT (Merotocin®), were reported to have achieved >1000-fold selectivity [62, 77]. All of these selective peptide analogs replaced proline at position 7 with glycine. This amino acid change is the basis of our selective peptides OXT^{Gly} and acylated-OXT^{Gly}, both of which achieved >1000-fold selectivity (Fig. 1). Furthermore, these two peptides demonstrated receptor selectivity *in vivo* as evidenced by the absence of an effect on blood pressure [67] or plasma electrolytes [67] following short-term and chronic administration, respectively. Aside from peptide analogs, nonpeptide OXTR agonists such as WAY-267464 and TC OT39 also showed a high degree of OXTR selectivity. However, these small-molecule agonists have significantly decreased potency (EC_{50}) and efficacy (E_{max}) in OXTR *in vitro* assays [67] (see also review by Manning *et al.* [62]). Additionally, these small-molecule agonists either have poor solubility or require special formulation and have low bioavailability ([78] and data not shown). Therefore, our long-acting and selective acylated-OXT^{Gly} is superior to current peptide and nonpeptide OXT analogs, as it exhibits strong potency, receptor selectivity *in vitro* and *in vivo*, preferable pharmacokinetics, is easy to formulate, and has a high degree of bioavailability.

Previous efforts have been made to extend the half-life of the OXT peptide. In particular, carbetocin (Duratocin®) offers protection against aminopeptidase degradation [79], thereby extending half-life to 40 to 80 minutes [70, 80], compared with 3 to 10 minutes for OXT in various species [70–72]. We did not find significant half-life extension for OXT^{Gly}, which is based on the aminopeptidase-resistant $OXT^{Butyryl}$ backbone [67] (Fig. 2). This could be due to the relatively long timescale of our pharmacokinetic study that did not have the resolution to distinguish small differences in half-life. Recently, lipidated OXT peptides were reported to have a long half-life and sustained effects on maternal and social behaviors for up to 24 hours in rats [81–83]. We experimented with attaching different lipid molecules (c18 diacid vs c16 monoacid) at distinct positions in the OXT peptide sequence (data not shown). Our approach allowed us to select for acylated peptides with the longest half-life while maintaining receptor activity and selectivity (Figs. 1 and 2 and data not shown). Importantly, OXT secretion is regulated by feed-forward self-stimulation [84]. Our current data have not addressed how prolonged exposure of OXT analogs (acylated-OXT and acylated-OXT^{Gly}) would affect endogenous OXT secretion.

We showed that OXT acutely suppressed food intake, confirming numerous previous reports [26, 28, 29, 31, 48]. In contrast, OXTR-selective OXT^{Gly} had a significantly reduced effect on food consumption whether injected peripherally or centrally [67] (Fig. 3). We further showed that OXT's effect on acute food suppression is abolished in the presence of the V1a and V2 inhibitor conivaptan (Fig. 3F). Our results suggest that native OXT activates the vasopressin receptor pathway *in vivo*, which contributes to the acute anorexigenic effect in mice. Consistent with these results, vasopressin was found to suppress food intake in rats [85], goats [86], and trout [87]. The anorexigenic response to vasopressin is likely secondary to the plasma osmolality imbalance mediated by V1 receptor activation [85]. Interestingly, direct activation of vasopressin neurons in the paraventricular hypothalamus also acutely inhibited food intake in mice [88]. Additionally, OXT-induced c-Fos expression in several brain regions that regulate appetite, including the paraventricular hypothalamus and nucleus of solitary tract, and was blocked by a vasopressin receptor (V1aR) antagonist (SR49059) [89]. We also observed that mice receiving central OXT (ICV) showed clinical signs of behavioral distress,

including high-pitched vocalization [67] and excessive grooming [67] during the first hour after injection. None of these behaviors was observed in either vehicle- or OXT^{Gly}-injected mice [67]. It is therefore likely that centrally administered OXT, but not OXT^{Gly}, causes behavioral distress, which may be partially responsible for the observed decrease in acute food intake. Taken together, these findings suggest a role for both peripheral and central vasopressin receptors in OXT-mediated control of food intake and stress response.

We observed a transient increase of MAP in OXT-injected rats, but not in OXT^{Gly}-injected rats, suggesting that vasopressin receptor activation by a nonselective OXT peptide contributed to a rise in MAP. Our result is consistent with a previous study showing a transient MAP increase minutes after IV OXT administration in rats [69]. Interestingly, this and other studies found a sustained decrease in blood pressure following daily SC OXT injections in rats [69, 90]. In addition to dose regimen and duration, OXT also exhibited differential blood pressure effects in different species. For example, IV OXT is well documented to cause transient hypotension in humans [91, 92] and monkeys [93], acute blood pressure increase in rats [94], and no blood pressure change in rabbits [93). Furthermore, OXT showed either beneficial or detrimental myocardial effects in different preclinical and clinical models [58–60, 95–97]. As these studies used nonselective OXT peptides, it is not clear whether the OXT or the vasopressin pathway mediated the hemodynamic and cardiovascular outcomes. Because cardiovascular effect is an important aspect for metabolic therapeutics, our selective and/or long-acting OXT analogs offer a valuable tool kit to help dissect pathway contributions to cardiovascular health in preclinical studies.

We found that both OXT and OXT^{Gly} attenuated the rise in blood glucose during an acute GTT (Fig. 4A and 4B), suggesting that activation of OXTR, rather than vasopressin receptors, modulates blood glucose. Our result is strikingly similar to a recent clinical study showing that nasal OXT treatment acutely reduced blood glucose in human subjects [51]. We further showed that OXT (2 mg/kg, IP) and OXT^{Gly} (2 mg/kg, IP) had a significantly stronger impact on glycemic control in obese mice than in lean mice (Fig. 4C). As the obese animals likely received higher dosages of OXT and OXT^{Gly} per lean mass compared with the lean animals, this may help explain the differential glycemic effects of OXT and its analogs in obese vs lean animals. Although clinical studies directly comparing the glycemic effect of OXT in humans with obesity vs lean humans have not been reported, one clinical study showed that OXT exhibited stronger suppression of food intake in human subjects with obesity, compared with lean human subjects, even though subjects with obesity received less nasal OXT per body weight [35]. Interestingly, an increase of circulating OXT level in response to insulin injection was documented, and the rise in OXT was impaired in men with obesity compared with lean men [98]. Together with these clinical observations, our results imply that OXT could have greater therapeutic efficacy in subjects with obesity, compared with lean subjects.

OXT and OXT^{Gly} modulate a combination of endocrine hormones and incretins, leading to the observed effect on blood glucose (Fig. 5). These peptides directly stimulated insulin secretion in isolated mouse but not human islets (Fig. 6A and 6B). This result is surprising because several studies demonstrated that OXT (IV or intranasal) led to an increased insulin level in human subjects [49–51]. It is therefore likely that insulin secretion stimulated by OXT occurs indirectly in humans. In contrast, glucagon was consistently stimulated by OXT analogs, both *in vivo* in mice (Fig. 5) and *ex vivo* in isolated human islets (Fig. 6). A similar glucagon effect was reported in multiple species, including rats, dogs, and humans [49, 99, 100]. In addition to insulin and glucagon, we also found a significant rise in circulating GLP-1 levels following OXT administration. This could be due to GLP-1 secretion from enteroendocrine cells triggered by the OXTR-expressing enteric neurons [101], or, alternatively, via other systemic hormonal changes. An increase of circulating GLP-1 could indirectly contribute to the rise of insulin levels following OXT administration in humans. Overall, our results provide a comprehensive view of likely mechanisms by which OXT modulates blood glucose. Interestingly, OXT's effect on glycemic control appears to be context-dependent: OXT promotes blood glucose rise upon fasting, whereas it decreases blood glucose during

hyperglycemia in human subjects [49]. Future work is needed to further investigate how OXT induces changes in hormones and incretins depending on glycemic status.

In contrast to the acute glycemic benefits, we did not observe improved glucose tolerance in mice chronically treated with OXT, acylated-OXT, or acylated-OXT^{Gly} (Fig. 7H) even though treated mice had significant weight loss. The difference in glycemic effects between acute and chronic treatments may be due to receptor sensitization, chronic changes in glucose regulating hormones, or other compensatory mechanisms. Interestingly, conflicting glycemic effects by chronic OXT treatment were reported with some showing benefits [24, 26], whereas others found worsening of glucose tolerance [53, 54]. Further studies are needed to investigate the likely causes of discrepancy such as species and age difference, animal models (DIO vs genetic obese), methods of GTT (ipGTT vs oral GTT), and duration and dosage of OXT treatment, among others. In comparison with the inconsistent glycemic effects observed in the rodent studies, a clinical weight loss study with chronic nasal OXT treatment showed a trend toward improvement of postprandial glucose and insulin [22].

We found significant weight loss in DIO mice treated with OXT analogs. In particular, the long-acting and nonselective acylated-OXT showed the most significant weight loss (Fig. 7A) when compared with native OXT, likely due to its superior pharmacokinetics (Fig. 2). Long-acting and selective acylated-OXT^{Gly} treatment also led to significant weight loss. However, the onset of weight loss following acylated-OXT^{Gly} treatment was slower than that observed with acylated-OXT treatment, suggesting a different mechanism of action. Intriguingly, acylated-OXT^{Gly} treatment resulted in the same amount of fat mass loss compared with acylated-OXT treatment, while preserving the lean mass (Fig. 7C). The possible engagement of vasopressin receptors and subsequent blood pressure rise [67] and ion imbalance [67] could explain the differential effects on acute food intake and chronic weight loss caused by OXTR-selective vs nonselective OXT analogs. Cholesterol and triglyceride lowering were similar between acylated-OXT and acylated OXT^{Gly}. Taken together, these results suggest that selective activation of the OXTR pathway has benefits on lipid metabolism and weight loss, whereas potential vasopressin pathway activation by nonselective OXT analogs causes physiological stresses such as increased blood pressure [67] and potassium ion imbalance [67], leading to additional lean mass loss. A selective reduction in fat mass would provide clinically meaningful weight loss, and therefore the acylated-OXT^{Gly} could be a valuable tool for future clinical investigations. Finally, OXT has a sex-specific role in reproduction, and we remain cautious regarding the translation of our results to human obesity treatment as our studies were done exclusively in male animals.

Acknowledgments

The authors thank the expert technical assistance of Janice Shaw, Matthew Hamang, Kimberly Ballman, and Chaohua Lin (Eli Lilly and Company). Additionally, the authors acknowledge Ruth Gimeno, Craig Hammond, and Julie Moyers (Eli Lilly and Company) for generous support of the project and input in the manuscript.

Author Contributions: M.A. designed the study with input from A.C.A., P.J.E., and J.A.-F. B.S. carried out all of the metabolic studies and related data analysis. A.G., L.G. and J.A.-F. synthesized the peptide analogs. X.-p.Y. performed the *in vitro* receptor screening. J.L. synthesized the small-molecule OXTR agonists. J.A.W. and Q.Y. conducted the pharmacokinetics studies. K.Q., X.W., E.C.B., and T.C. performed the hemodynamic study in rats. A.E. did the *ex vivo* islet studies. M.A., P.J.E., and J.A.F. wrote the manuscript with input from all authors.

Current Affiliation: J.L.'s current affiliation is Novartis Institute for BioMedical Research, Cambridge, Massachusetts 02139. Q.Y.'s current affiliation is GlaxoSmithKline, Collegeville, Pennsylvania 19426.

Correspondence: Minrong Ai, PhD, Diabetes and Complications, Lilly Research Laboratories, Eli Lilly and Company, 639 South Delaware Street, Indianapolis, Indiana 46285. E-mail: ai_minrong@lilly.com; or Jorge Alsina-Fernandez, Biotechnology Peptide Group, Lilly Research Laboratories, Eli Lilly and Company, 639 South Delaware Street, Indianapolis, Indiana 46285. E-mail: alsina-fernandez_jorge@lilly.com.

Prior presentation: Selected results reported herein were presented as a poster at the Keystone Symposia, Organ Crosstalk in Obesity and NAFLD (J3), 21–25 January 2018, Keystone, Colorado.

Disclosure Summary: B.S., A.G., X.-p.Y., E.C.B., J.A.W., K.Q., L.G., J.L., X.W., Q.Y., A.E., A.C.A., T.C., P.J.E., J.A.-F, and M.A. are either current or past employees of Eli Lilly and Company and may own company stock or possess stock options.

References and Notes

1. Kimura T, Ogita K, Kumasawa K, Tomimatsu T, Tsutsui T. Molecular analysis of parturition via oxytocin receptor expression. *Taiwan J Obstet Gynecol*. 2013;**52**(2):165–170.
2. Fuchs AR, Fuchs F, Husslein P, Soloff MS. Oxytocin receptors in the human uterus during pregnancy and parturition. *Am J Obstet Gynecol*. 1984;**150**(6):734–741.
3. Breton C, Di Scala-Guenot D, Zingg HH. Oxytocin receptor gene expression in rat mammary gland: structural characterization and regulation. *J Mol Endocrinol*. 2001;**27**(2):175–189.
4. Marlin BJ, Mitre M, D'amour JA, Chao MV, Froemke RC. Oxytocin enables maternal behaviour by balancing cortical inhibition. *Nature*. 2015;**520**(7548):499–504.
5. Pedersen CA, Prange AJ Jr. Induction of maternal behavior in virgin rats after intracerebroventricular administration of oxytocin. *Proc Natl Acad Sci USA*. 1979;**76**(12):6661–6665.
6. Pedersen CA, Ascher JA, Monroe YL, Prange AJ Jr. Oxytocin induces maternal behavior in virgin female rats. *Science*. 1982;**216**(4546):648–650.
7. Cushing BS, Carter CS. Peripheral pulses of oxytocin increase partner preferences in female, but not male, prairie voles. *Horm Behav*. 2000;**37**(1):49–56.
8. Insel TR, Hulihan TJ. A gender-specific mechanism for pair bonding: oxytocin and partner preference formation in monogamous voles. *Behav Neurosci*. 1995;**109**(4):782–789.
9. Kosfeld M, Heinrichs M, Zak PJ, Fischbacher U, Fehr E. Oxytocin increases trust in humans. *Nature*. 2005;**435**(7042):673–676.
10. Rimmele U, Hediger K, Heinrichs M, Klaver P. Oxytocin makes a face in memory familiar. *J Neurosci*. 2009;**29**(1):38–42.
11. Preti A, Melis M, Siddi S, Vellante M, Doneddu G, Fadda R. Oxytocin and autism: a systematic review of randomized controlled trials. *J Child Adolesc Psychopharmacol*. 2014;**24**(2):54–68.
12. Oxytocin trial in Prader-Willi syndrome. Available at: https://ClinicalTrials.gov/show/NCT02013258. Accessed 1 August 2015.
13. Oxytocin intranasal administrations in children with Prader-Willi syndrome aged from 3 to 12 years. Available at: https://ClinicalTrials.gov/show/NCT03114371. Accessed 1 December 2018.
14. Intranasal oxytocin for infants with Prader-Willi syndrome. Available at: https://ClinicalTrials.gov/show/NCT03245762. Accessed 1 December 2018.
15. Oxytocin vs. placebo for the treatment hyperphagia in children and adolescents with Prader-Willi syndrome. Available at: https://ClinicalTrials.gov/show/NCT02629991. April, 2018
16. Goodin BR, Ness TJ, Robbins MT. Oxytocin—a multifunctional analgesic for chronic deep tissue pain. *Curr Pharm Des*. 2015;**21**(7):906–913.
17. Efficacy of intrathecal oxytocin in patients with neuropathic pain. Available at: https://ClinicalTrials.gov/show/NCT02100956. Accessed 1 May 2019.
18. Oxytocin treatment of alcohol dependence. Available at: https://ClinicalTrials.gov/show/NCT02251912. Accessed 1 August 2017.
19. Oxytocin treatment of alcohol withdrawal. Available at: https://ClinicalTrials.gov/show/NCT01212185. Accessed 1 May 2014.
20. Oxytocin and alcohol withdrawal and dependence. Available at: https://ClinicalTrials.gov/show/NCT02903251. Accessed 1 February 2019.
21. Pedersen CA, Smedley KL, Leserman J, Jarskog LF, Rau SW, Kampov-Polevoi A, Casey RL, Fender T, Garbutt JC. Intranasal oxytocin blocks alcohol withdrawal in human subjects. *Alcohol Clin Exp Res*. 2013;**37**(3):484–489.
22. Zhang H, Wu C, Chen Q, Chen X, Xu Z, Wu J, Cai D. Treatment of obesity and diabetes using oxytocin or analogs in patients and mouse models. *PLoS One*. 2013;**8**(5):e61477.
23. Blevins JE, Graham JL, Morton GJ, Bales KL, Schwartz MW, Baskin DG, Havel PJ. Chronic oxytocin administration inhibits food intake, increases energy expenditure, and produces weight loss in fructose-fed obese rhesus monkeys. *Am J Physiol Regul Integr Comp Physiol*. 2015;**308**(5):R431–R438.

24. Deblon N, Veyrat-Durebex C, Bourgoin L, Caillon A, Bussier AL, Petrosino S, Piscitelli F, Legros JJ, Geenen V, Foti M, Wahli W, Di Marzo V, Rohner-Jeanrenaud F. Mechanisms of the anti-obesity effects of oxytocin in diet-induced obese rats. *PLoS One*. 2011;**6**(9):e25565.
25. Ho JM, Anekonda VT, Thompson BW, Zhu M, Curry RW, Hwang BH, Morton GJ, Schwartz MW, Baskin DG, Appleyard SM, Blevins JE. Hindbrain oxytocin receptors contribute to the effects of circulating oxytocin on food intake in male rats. *Endocrinology*. 2014;**155**(8):2845–2857.
26. Maejima Y, Iwasaki Y, Yamahara Y, Kodaira M, Sedbazar U, Yada T. Peripheral oxytocin treatment ameliorates obesity by reducing food intake and visceral fat mass. *Aging (Albany NY)*. 2011;**3**(12): 1169–1177.
27. Maejima Y, Takahashi S, Takasu K, Takenoshita S, Ueta Y, Shimomura K. Orexin action on oxytocin neurons in the paraventricular nucleus of the hypothalamus. *Neuroreport*. 2017;**28**(6):360–366.
28. Arletti R, Benelli A, Bertolini A. Influence of oxytocin on feeding behavior in the rat. *Peptides*. 1989; **10**(1):89–93.
29. Olson BR, Drutarosky MD, Chow MS, Hruby VJ, Stricker EM, Verbalis JG. Oxytocin and an oxytocin agonist administered centrally decrease food intake in rats. *Peptides*. 1991;**12**(1):113–118.
30. Roberts ZS, Wolden-Hanson T, Matsen ME, Ryu V, Vaughan CH, Graham JL, Havel PJ, Chukri DW, Schwartz MW, Morton GJ, Blevins JE. Chronic hindbrain administration of oxytocin is sufficient to elicit weight loss in diet-induced obese rats. *Am J Physiol Regul Integr Comp Physiol*. 2017;**313**(4): R357–R371.
31. Blevins JE, Thompson BW, Anekonda VT, Ho JM, Graham JL, Roberts ZS, Hwang BH, Ogimoto K, Wolden-Hanson T, Nelson J, Kaiyala KJ, Havel PJ, Bales KL, Morton GJ, Schwartz MW, Baskin DG. Chronic CNS oxytocin signaling preferentially induces fat loss in high-fat diet-fed rats by enhancing satiety responses and increasing lipid utilization. *Am J Physiol Regul Integr Comp Physiol*. 2016; **310**(7):R640–R658.
32. Ott V, Finlayson G, Lehnert H, Heitmann B, Heinrichs M, Born J, Hallschmid M. Oxytocin reduces reward-driven food intake in humans. *Diabetes*. 2013;**62**(10):3418–3425.
33. Lawson EA, Marengi DA, DeSanti RL, Holmes TM, Schoenfeld DA, Tolley CJ. Oxytocin reduces caloric intake in men. *Obesity (Silver Spring)*. 2015;**23**(5):950–956.
34. Spetter MS, Feld GB, Thienel M, Preissl H, Hege MA, Hallschmid M. Oxytocin curbs calorie intake via food-specific increases in the activity of brain areas that process reward and establish cognitive control. *Sci Rep*. 2018;**8**(1):2736.
35. Thienel M, Fritsche A, Heinrichs M, Peter A, Ewers M, Lehnert H, Born J, Hallschmid M. Oxytocin's inhibitory effect on food intake is stronger in obese than normal-weight men. *Int J Obes*. 2016;**40**(11): 1707–1714.
36. van der Klaauw AA, Ziauddeen H, Keogh JM, Henning E, Dachi S, Fletcher PC, Farooqi IS. Oxytocin administration suppresses hypothalamic activation in response to visual food cues. *Sci Rep*. 2017;**7**(1): 4266.
37. Plessow F, Marengi DA, Perry SK, Felicione JM, Franklin R, Holmes TM, Holsen LM, Makris N, Deckersbach T, Lawson EA. Effects of intranasal oxytocin on the blood oxygenation level-dependent signal in food motivation and cognitive control pathways in overweight and obese men. *Neuropsychopharmacology*. 2018;**43**(3):638–645.
38. Hsu EA, Miller JL, Perez FA, Roth CL. Oxytocin and naltrexone successfully treat hypothalamic obesity in a boy post-craniopharyngioma resection. *J Clin Endocrinol Metab*. 2018;**103**(2):370–375.
39. Fenselau H, Campbell JN, Verstegen AM, Madara JC, Xu J, Shah BP, Resch JM, Yang Z, Mandelblat-Cerf Y, Livneh Y, Lowell BB. A rapidly acting glutamatergic ARC→PVH satiety circuit post-synaptically regulated by α-MSH [published correction appears in *Nat Neurosci*. 2017;**20**(8):1189]. *Nat Neurosci*. 2017;**20**(1):42–51.
40. Noble EE, Billington CJ, Kotz CM, Wang C. Oxytocin in the ventromedial hypothalamic nucleus reduces feeding and acutely increases energy expenditure. *Am J Physiol Regul Integr Comp Physiol*. 2014;**307**(6):R737–R745.
41. Ong ZY, Alhadeff AL, Grill HJ. Medial nucleus tractus solitarius oxytocin receptor signaling and food intake control: the role of gastrointestinal satiation signal processing. *Am J Physiol Regul Integr Comp Physiol*. 2015;**308**(9):R800–R806.
42. Mullis K, Kay K, Williams DL. Oxytocin action in the ventral tegmental area affects sucrose intake. *Brain Res*. 2013;**1513**:85–91.
43. Kasahara Y, Sato K, Takayanagi Y, Mizukami H, Ozawa K, Hidema S, So KH, Kawada T, Inoue N, Ikeda I, Roh SG, Itoi K, Nishimori K. Oxytocin receptor in the hypothalamus is sufficient to rescue normal thermoregulatory function in male oxytocin receptor knockout mice. *Endocrinology*. 2013; **154**(11):4305–4315.

44. Kasahara Y, Takayanagi Y, Kawada T, Itoi K, Nishimori K. Impaired thermoregulatory ability of oxytocin-deficient mice during cold-exposure. *Biosci Biotechnol Biochem*. 2007;**71**(12):3122–3126.
45. Xi D, Long C, Lai M, Casella A, O'Lear L, Kublaoui B, Roizen JD. Ablation of oxytocin neurons causes a deficit in cold stress response. *J Endocr Soc*. 2017;**1**(8):1041–1055.
46. Ong ZY, Bongiorno DM, Hernando MA, Grill HJ. Effects of endogenous oxytocin receptor signaling in nucleus tractus solitarius on satiation-mediated feeding and thermogenic control in male rats. *Endocrinology*. 2017;**158**(9):2826–2836.
47. Wu Z, Xu Y, Zhu Y, Sutton AK, Zhao R, Lowell BB, Olson DP, Tong Q. An obligate role of oxytocin neurons in diet induced energy expenditure. *PLoS One*. 2012;**7**(9):e45167.
48. Zhang G, Bai H, Zhang H, Dean C, Wu Q, Li J, Guariglia S, Meng Q, Cai D. Neuropeptide exocytosis involving synaptotagmin-4 and oxytocin in hypothalamic programming of body weight and energy balance. *Neuron*. 2011;**69**(3):523–535.
49. Paolisso G, Sgambato S, Passariello N, Torella R, Giugliano D, Mignano S, Varricchio M, D'Onofrio F. Pharmacological doses of oxytocin affect plasma hormone levels modulating glucose homeostasis in normal man. *Horm Res*. 1988;**30**(1):10–16.
50. Paolisso G, Sgambato S, Passariello N, Giugliano D, Torella R, Memoli P, Varricchio M, D'Onofrio F. Oxytocin increases arginine-induced A and B cell secretion in normal man and in diabetic subjects. *Diabete Metab*. 1988;**14**(2):104–107.
51. Klement J, Ott V, Rapp K, Brede S, Piccinini F, Cobelli C, Lehnert H, Hallschmid M. Oxytocin improves β-cell responsivity and glucose tolerance in healthy men. *Diabetes*. 2017;**66**(2):264–271.
52. Vilhardt H, Krarup T, Holst JJ, Bie P. The mechanism of the effect of oxytocin on plasma concentrations of glucose, insulin and glucagon in conscious dogs. *J Endocrinol*. 1986;**108**(2):293–298.
53. Altirriba J, Poher AL, Caillon A, Arsenijevic D, Veyrat-Durebex C, Lyautey J, Dulloo A, Rohner-Jeanrenaud F. Divergent effects of oxytocin treatment of obese diabetic mice on adiposity and diabetes. *Endocrinology*. 2014;**155**(11):4189–4201.
54. Balazova L, Krskova K, Suski M, Sisovsky V, Hlavacova N, Olszanecki R, Jezova D, Zorad S. Metabolic effects of subchronic peripheral oxytocin administration in lean and obese zucker rats. *J Physiol Pharmacol*. 2016;**67**(4):531–541.
55. Beranger GE, Pisani DF, Castel J, Djedaini M, Battaglia S, Amiaud J, Boukhechba F, Ailhaud G, Michiels JF, Heymann D, Luquet S, Amri EZ. Oxytocin reverses ovariectomy-induced osteopenia and body fat gain. *Endocrinology*. 2014;**155**(4):1340–1352.
56. Elabd C, Cousin W, Upadhyayula P, Chen RY, Chooljian MS, Li J, Kung S, Jiang KP, Conboy IM. Oxytocin is an age-specific circulating hormone that is necessary for muscle maintenance and regeneration. *Nat Commun*. 2014;**5**(1):4082.
57. Yuan L, Liu S, Bai X, Gao Y, Liu G, Wang X, Liu D, Li T, Hao A, Wang Z. Oxytocin inhibits lipopolysaccharide-induced inflammation in microglial cells and attenuates microglial activation in lipopolysaccharide-treated mice. *J Neuroinflammation*. 2016;**13**(1):77.
58. Plante E, Menaouar A, Danalache BA, Yip D, Broderick TL, Chiasson JL, Jankowski M, Gutkowska J. Oxytocin treatment prevents the cardiomyopathy observed in obese diabetic male db/db mice. *Endocrinology*. 2015;**156**(4):1416–1428.
59. Menaouar A, Florian M, Wang D, Danalache B, Jankowski M, Gutkowska J. Anti-hypertrophic effects of oxytocin in rat ventricular myocytes. *Int J Cardiol*. 2014;**175**(1):38–49.
60. Kobayashi H, Yasuda S, Bao N, Iwasa M, Kawamura I, Yamada Y, Yamaki T, Sumi S, Ushikoshi H, Nishigaki K, Takemura G, Fujiwara T, Fujiwara H, Minatoguchi S. Postinfarct treatment with oxytocin improves cardiac function and remodeling via activating cell-survival signals and angiogenesis. *J Cardiovasc Pharmacol*. 2009;**54**(6):510–519.
61. Gonzalez-Reyes A, Menaouar A, Yip D, Danalache B, Plante E, Noiseux N, Gutkowska J, Jankowski M. Molecular mechanisms underlying oxytocin-induced cardiomyocyte protection from simulated ischemia-reperfusion. *Mol Cell Endocrinol*. 2015;**412**:170–181.
62. Manning M, Misicka A, Olma A, Bankowski K, Stoev S, Chini B, Durroux T, Mouillac B, Corbani M, Guillon G. Oxytocin and vasopressin agonists and antagonists as research tools and potential therapeutics. *J Neuroendocrinol*. 2012;**24**(4):609–628.
63. Gehlert DR, Cramer J, Morin SM. Effects of corticotropin-releasing factor 1 receptor antagonism on the hypothalamic-pituitary-adrenal axis of rodents. *J Pharmacol Exp Ther*. 2012;**341**(3):672–680.
64. RRID:AB_2801382. http://antibodyregistry.org/search.php?q=AB_2801382.
65. RRID:AB_2801383. http://antibodyregistry.org/search.php?q=AB_2801383.
66. RRID:AB_2801384. http://antibodyregistry.org/search.php?q=AB_2801384.
67. Snider B, Geiser A, Yu XP, Beebe EC, Willency JA, Qing K, Guo L, Lu J, Wang X, Yang Q, Efanov A, Adams AC, Coskun T, Emmerson PJ, Alsina-Fernandez J, Ai M. Data from: Long-acting and selective

oxytocin peptide analogs show antidiabetic and antiobesity effects in male mice. Dryad 2019. https://doi.org/10.5061/dryad.jk21h17. Accessed 1 May 2019.
68. den Ouden DT, Meinders AE. Vasopressin: physiology and clinical use in patients with vasodilatory shock: a review. *Neth J Med*. 2005;**63**(1):4–13.
69. Gutkowska J, Aliou Y, Lavoie JL, Gaab K, Jankowski M, Broderick TL. Oxytocin decreases diurnal and nocturnal arterial blood pressure in the conscious unrestrained spontaneously hypertensive rat. *Pathophysiology*. 2016;**23**(2):111–121.
70. Sweeney G, Holbrook M, Levine M, Yip M, Alfredsson K, Cappi S, Ohlin M, Schulz P, Wassenaar W. Pharmacokinetics of carbetocin, a long-acting oxytocin analogue, in nonpregnant women. *Curr Ther Res Clin Exp*. 1990;**47**(3):528–540.
71. Gazis D. Plasma half-lives of vasopressin and oxytocin analogs after iv injection in rats. *Proc Soc Exp Biol Med*. 1978;**158**(4):663–665.
72. Freeman SM, Samineni S, Allen PC, Stockinger D, Bales KL, Hwa GG, Roberts JA. Plasma and CSF oxytocin levels after intranasal and intravenous oxytocin in awake macaques. *Psychoneuroendocrinology*. 2016;**66**:185–194.
73. Schweiger TA, Zdanowicz MM. Vasopressin-receptor antagonists in heart failure. *Am J Health Syst Pharm*. 2008;**65**(9):807–817.
74. Morton GJ, Thatcher BS, Reidelberger RD, Ogimoto K, Wolden-Hanson T, Baskin DG, Schwartz MW, Blevins JE. Peripheral oxytocin suppresses food intake and causes weight loss in diet-induced obese rats. *Am J Physiol Endocrinol Metab*. 2012;**302**(1):E134–E144.
75. Elalouf JM, Roinel N, de Rouffignac C. Effects of antidiuretic hormone on electrolyte reabsorption and secretion in distal tubules of rat kidney. *Pflugers Arch*. 1984;**401**(2):167–173.
76. Kutina AV, Marina AS, Shakhmatova EI, Natochin YV. Vasotocin analogues with selective natriuretic, kaliuretic and antidiuretic effects in rats. *Regul Pept*. 2013;**185**:57–64.
77. Wiśniewski K, Alagarsamy S, Galyean R, Tariga H, Thompson D, Ly B, Wiśniewska H, Qi S, Croston G, Laporte R, Rivière PJ, Schteingart CD. New, potent, and selective peptidic oxytocin receptor agonists. *J Med Chem*. 2014;**57**(12):5306–5317.
78. Ring RH, Schechter LE, Leonard SK, Dwyer JM, Platt BJ, Graf R, Grauer S, Pulicicchio C, Resnick L, Rahman Z, Sukoff Rizzo SJ, Luo B, Beyer CE, Logue SF, Marquis KL, Hughes ZA, Rosenzweig-Lipson S. Receptor and behavioral pharmacology of WAY-267464, a non-peptide oxytocin receptor agonist. *Neuropharmacology*. 2010;**58**(1):69–77.
79. Barth T, Krejcí I, Vaněcková J, Jost K, Rychlík I. Prolonged action of deamino-carba analogues of oxytocin on the rat uterus in vivo. *Eur J Pharmacol*. 1974;**25**(1):67–70.
80. Cort N, Einarsson S, Schams D, Vilhardt H. Blood concentrations of oxytocin equivalents after single injections of deamino-1-monocarba-[2-*O*-methyltyrosine]-oxytocin in lactating sows. *Am J Vet Res*. 1981;**42**(10):1804–1806.
81. Cherepanov SM, Akther S, Nishimura T, Shabalova AA, Mizuno A, Ichinose W, Shuto S, Yamamoto Y, Yokoyama S, Higashida H. Effects of three lipidated oxytocin analogs on behavioral deficits in CD38 knockout mice. *Brain Sci*. 2017;**7**(10):E132.
82. Cherepanov SM, Yokoyama S, Mizuno A, Ichinose W, Lopatina O, Shabalova AA, Salmina AB, Yamamoto Y, Okamoto H, Shuto S, Higashida H. Structure-specific effects of lipidated oxytocin analogs on intracellular calcium levels, parental behavior, and oxytocin concentrations in the plasma and cerebrospinal fluid in mice. *Pharmacol Res Perspect*. 2017;**5**(1):e00290.
83. Mizuno A, Cherepanov SM, Kikuchi Y, Fakhrul AA, Akther S, Deguchi K, Yoshihara T, Ishihara K, Shuto S, Higashida H. Lipo-oxytocin-1, a novel oxytocin analog conjugated with two palmitoyl groups, has long-lasting effects on anxiety-related behavior and social avoidance in CD157 knockout mice. *Brain Sci*. 2015;**5**(1):3–13.
84. Ludwig M, Sabatier N, Bull PM, Landgraf R, Dayanithi G, Leng G. Intracellular calcium stores regulate activity-dependent neuropeptide release from dendrites. *Nature*. 2002;**418**(6893):85–89.
85. Ikemura R, Matsuwaki T, Yamanouchi K, Nishihara M. Involvement of endogenous vasopressin in high plasma osmolality-induced anorexia via V1 receptor-mediated mechanism. *J Vet Med Sci*. 2004; **66**(8):951–955.
86. Meyer AH, Langhans W, Scharrer E. Vasopressin reduces food intake in goats. *Q J Exp Physiol*. 1989; **74**(4):465–473.
87. Gesto M, Soengas JL, Rodríguez-Illamola A, Míguez JM. Arginine vasotocin treatment induces a stress response and exerts a potent anorexigenic effect in rainbow trout, *Oncorhynchus mykiss*. *J Neuroendocrinol*. 2014;**26**(2):89–99.
88. Pei H, Sutton AK, Burnett KH, Fuller PM, Olson DP. AVP neurons in the paraventricular nucleus of the hypothalamus regulate feeding. *Mol Metab*. 2014;**3**(2):209–215.

89. Hicks C, Ramos L, Dampney B, Baracz SJ, McGregor IS, Hunt GE. Regional c-Fos expression induced by peripheral oxytocin administration is prevented by the vasopressin 1A receptor antagonist SR49059. *Brain Res Bull*. 2016;**127**:208–218.
90. Petersson M, Alster P, Lundeberg T, Uvnäs-Moberg K. Oxytocin causes a long-term decrease of blood pressure in female and male rats. *Physiol Behav*. 1996;**60**(5):1311–1315.
91. Thomas JS, Koh SH, Cooper GM. Haemodynamic effects of oxytocin given as i.v. bolus or infusion on women undergoing Caesarean section. *Br J Anaesth*. 2007;**98**(1):116–119.
92. Bhattacharya S, Ghosh S, Ray D, Mallik S, Laha A. Oxytocin administration during cesarean delivery: randomized controlled trial to compare intravenous bolus with intravenous infusion regimen. *J Anaesthesiol Clin Pharmacol*. 2013;**29**(1):32–35.
93. Hess L, Votava M, Málek J, Kurzová A, Slíva J. Sedative effects of intranasal oxytocin in rabbits and rhesus monkeys. *Physiol Res*. 2016;**65**(Suppl 4):S473–S480.
94. Petersson M, Lundeberg T, Uvnäs-Moberg K. Short-term increase and long-term decrease of blood pressure in response to oxytocin-potentiating effect of female steroid hormones. *J Cardiovasc Pharmacol*. 1999;**33**(1):102–108.
95. Svanström MC, Biber B, Hanes M, Johansson G, Näslund U, Bålfors EM. Signs of myocardial ischaemia after injection of oxytocin: a randomized double-blind comparison of oxytocin and methylergometrine during Caesarean section. *Br J Anaesth*. 2008;**100**(5):683–689.
96. Phie J, Haleagrahara N, Newton P, Constantinoiu C, Sarnyai Z, Chilton L, Kinobe R. Prolonged subcutaneous administration of oxytocin accelerates angiotensin ii-induced hypertension and renal damage in male rats. *PLoS One*. 2015;**10**(9):e0138048.
97. Morris M, Callahan MF, Li P, Lucion AB. Central oxytocin mediates stress-induced tachycardia. *J Neuroendocrinol*. 1995;**7**(6):455–459.
98. Coiro V, Passeri M, Davoli C, d'Amato L, Gelmini G, Fagnoni F, Schianchi L, Bentivoglio M, Volpi R, Chiodera P. Oxytocin response to insulin-induced hypoglycemia in obese subjects before and after weight loss. *J Endocrinol Invest*. 1988;**11**(2):125–128.
99. Altszuler N, Winkler B, Rosenberg CR, Pi-Sunyer FX, Fuchs AR. Role of insulin and glucagon in oxytocin effects on glucose metabolism. *Proc Soc Exp Biol Med*. 1992;**199**(2):236–242.
100. Widmaier EP, Shah PR, Lee G. Interactions between oxytocin, glucagon and glucose in normal and streptozotocin-induced diabetic rats. *Regul Pept*. 1991;**34**(3):235–249.
101. Welch MG, Tamir H, Gross KJ, Chen J, Anwar M, Gershon MD. Expression and developmental regulation of oxytocin (OT) and oxytocin receptors (OTR) in the enteric nervous system (ENS) and intestinal epithelium. *J Comp Neurol*. 2009;**512**(2):256–270.